# Possible Therapeutic Effect of Gene Modified Versus Non-Modified Stem Cells on Hippocampus and Cerebral Cortex in Alzheimer's Female Albino Rat Model Complicating Experimentally Induced Diabetes Type I

Original Article

*Maha Baligh Zickri[1,2], Hala Gabr Metwally[3], Omaima Mohamed Abdelwahed[4], Mai Abdelaziz Gouda[5,6], Rokia Mohamad Hassan[1], Shaimaa Ahmed Zaki[1] and Alshaymaa Gamal Aboulkhair[1]*

*[1]Department of Medical Histology & Cell Biology, [3]Department of Clinical Pathology, [4]Department of Medical Physiology, Faculty of Medicine, Cairo University, [2]Faculty of Oral and Dental Medicine, Future University, Egypt (FUE)*

*Department of Medical Biochemistry & Molecular Biology, Faculty of Medicine, [5]Cairo University, [6]Badr University in Cairo*

## ABSTRACT

**Introduction and Objectives:** The relation linking type1 diabetes (T1DM) to Alzheimer's disease (AD) was recorded. Recently, widespread attention for gene modification of stem cells (SCs) was established. The present work aimed at investigating possible ameliorating impact of gene modified SCs on cerebral cortex and hippocampus in Alzheimer's disease (AD) complicating T1DM.

**Methods and Results:** 40 female rats were classified into: In *Vitro* Study Group: 4 animals used to perform SCs culture and Sarco-Endoplasmic Reticulum $Ca^{2+}$ATPase (SERCA) 2b preparation. Control Group (A): 6 animals. Diabetic Group (B): 10 animals received IP injection 50 mg/kg streptozotocin (STZ). Non-transfected SCs Group (C): 10 rats, received 1×106 rat SCs intravenous. SERCA2b transfected SCs Group (D): 10 rats received 1x106 transfected SCs. 52 days after proving incidence of diabetes, neurological, serum glucose, morphological, morphometric, gene quantitation, western blot and biochemical studies were performed. Neurological study expressed a decrease in group B and in group C. Group B clarified degenerated neurons in external pyramidal (EP) layer and dentate gyrus (DG). Group D revealed more obvious regression of degenerative changes than group C. An increase in area of deformed nerve cells and Congo red +ve neurons, mean area% of immunoexpression (IE) were found in groups B and C. Mean Ca ion concentration, catalase, SERCA2b gene and protein values expressed a significant (sig) decrease in groups B and C. Mean MDA and beta amyloid protein proved a sig increase in groups B and C.

**Conclusions:** Stem cells transfected with sarcoplasmic reticulum calcium ATPase2b gene proved pronounced therapeutic impact suggesting its potency and regenerative capacity in remarkable amelioration of Alzheimer's disease complicating diabetes I.

**Received:** 28 Novamber 2022, **Accepted:** 03 January 2023

**Key Words:** AMSCs, caspase3, catalase, GFAP, MDA, qPCR, SERCA, T1DM, Wb.

**Corresponding Author:** Shaimaa Ahmed Zaki Ahmed, MD, Department of Medical Histology & Cell Biology, Faculty of Medicine, Cairo University, Egypt, **Tel.**: +20 10 0523 5117, **E-mail:** shimaa24_smile7@cu.edu.eg

**ISSN:** 1110-0559, Vol. 47, No. 1

## INTRODUCTION

Recent studies have suggested a link between T1DM and high intellectual cerebral functions[1]. Chronic hyperglycemia is closely related to development of cognitive impairment associated with AD[2]. Prestia *et al*[3] mentioned that AD is associated to impaired cortical and hippocampal synaptic function.

Cao *et al*[4] reported that, most of medications used in the treatment of AD proved minimal therapeutic efficacy. Recent therapeutic modalities are required to limit progression of AD. Administration of stem cells of mesenchymal origin proved to transdifferentiate into damaged neurons in progressive neurodegenerative diseases[5]. Recently, adipose derived MSCs (AMSCs) proved as alternative to other MSCs[6].

The calcium ion ($Ca^{2+}$) signaling has an important impact on structural and functional properties of neurons. Changes of $Ca^{2+}$ content homeostasis were crucial in neurodegenerative disorders, including AD[7]. Recently, gene modification of MSCs in different tissue cultures[8] was established. Sarco-endoplasmic reticulum $Ca^{2+}$-ATPase 2b (SERCA2b) is gene coding for SERCA2b integral protein of endoplasmic reticulum (ER) that preserves low cytosolic $Ca^{2+}$ levels[9].

 *DOI: 10.21608/ejh.2023.177550.1824*

The present work aimed at investigating possible ameliorating impact of SERCA2b gene modified AMSCs versus non-modified AMSCs on morphological changes in cerebral cortex and hippocampus of AD female albino rat model complicating T1DM. Neurological, serological, morphometric, polymerase chain reaction, western blot and biochemical confirmative studies were performed.

## MATERIALS AND METHODS

### *Experimental Design*

Forty adult female albino rats weighing 200-220 grams were kept in a well-ventilated room and kept in hygienic cages in the Animal House, Faculty of Medicine, Cairo University. Animal Ethics Committee of Cairo University approved all procedures with approval number: 34 20. The animals were randomly classified into:

In *Vitro* Study Group: Using four animals to obtain SCs, perform culture, phenotyping and labeling. In addition, the brain was homogenized and processed for SERCA2b preparation by reverse transcription[10]. The above mentioned procedures were accomplished at the Hematology Unit.

**Group A** (Control Group): six animals, the 1st two were injected intraperitoneal (IP) once with 0.5 ml citrate buffer (CB). For the 2nd two, 24 days following CB injection, 1ml of phosphate buffered saline (PBS) was injected intravenous (IV). The 3rd two were injected IV with 1.5 µl lipofectamine in addition, 24 days following CB injection.

**Group B** (Diabetic Group): 10 animals were injected IP with STZ (Sigma, USA). 50 mg/kg was dissolved for each animal in 0.5 ml CB once[1]. Assessment of serum glucose value was performed 3 days after STZ administration, to confirm diabetes in Clinical Chemistry Unit. Diabetes was diagnosed by a level higher than 200 mg/dl. The animals that didn't reach the glycemic target were excluded from the study[11]. The animals of this group were left without treatment till time of sacrifice.

**Group C** (AMSCs Group): 10 animals. On the 24$^{th}$ day, 1x106 of propagated and Feridex tagged rat AMSCs[12], preserved in one ml PBS and injected IV[13].

**Group D** (Gene modified AMSCs Group): 10 animals. On the 24th day, 1x106 of propagated and green fluorescent protein (GFP) tagged[14] SERCA2b modified AMSCs were injected IV.

The rats of all groups were euthanised 52 days from the start of the experiment.

### *Rat derived AMSCs collection and culture*[15]

Carbon dioxide (CO2) was used to sacrifice the animals. Abdominal fatty tissues were isolated under sterile conditions and cultured in DMEM (Dulbecco's Modified Eagle's Medium) (GIBCO/BRL). After centrifugation, the lowest layer was obtained. Resuspension of cells was done in DMEM supplemented with 1% antibiotic and bovine serum at 37 °C for 2 weeks. AMSCs were detached using enzyme in ethylene diaminetetraacetic acid. Following recentrifugation, SCs were placed and cultured in Falcon flask. 4th passage cultures were completed in Hematology Unit.

### *Characterization of AMSCs and flow cytometry*

10µl of CD34 (14-0341-81, RAM34) and 10µl of CD105 (MA5-11854, SN6h), (Thermo Fisher Scientific, USA) (Immunocytochemical characterization) were applied for 20 mintes[16]. Cell percentage was assessed by Flow Cytometer (FC) 500 (Beckman coulter, USA) and determined by CXP Software in Hematology Unit.

### *Labeling of AMSCs with Feridex*[12]

In culture medium, non-modified SCs were tagged by Feridex (25microgram ferrumoxide/ml, Berlex Labs) for 1day. Labeling was demonstrated by Prussian blue stain. Plasticity and regenerative capacity of tagged cells are preserved.

Transfection[17] and tagging[14] of SERCA2b modified AMSCs and flow cytometry

In DMEM culture medium, 1.5 µl Lipofectamine 3000 solution and 1.5 µg SERCA2b tagged with GFP were added. GFP attaches to loci on the gene. Examination of tagging was performed using fluorescent microscopy. SERCA2b transfected AMSCs were examined using FC percentage determination.

### *Animal Studies*

**Neurological screening and behavioral testing**[18]

The Y-maze test: measures memory for space. Three similar arms made up the equipment. For 8 minutes, each animal was kept in the centre. To test their memory, rats often alternate between the three arms. An arm entry was considered successful when the rat placed all four paws inside that arm. The ratio of the actual to the maximum number of alternations was used to calculate the alternation %. The total number of arm entries minus two was used to determine the maximum number of alternations that could be made. Low% suggests a problem with spatial memory.

The open field (OF) test: to determine locomotor activity, exploratory activity and behavior related to anxiety. The equipment was formed of white wood with central square area. Video camera was installed in a quiet illuminated room, the behavior of each animal was evaluated for 10 min after placing in central square area. All fecal pellets and all spots of urination were wiped up. The quadrant was sprayed with 70% ethanol. The followings were recorded: 1. number of lines crossed by four paws of rat. 2. Rearing behavior: frequency of rats standing on their hind limbs to assess locomotor activity, exploration and anxiety behavior. 3. Total number of entries to center of open field. 4. Time spent in central part to assess anxiety levels.

### *Serological Study*

Was performed for serum sugar level estimation 52 days from start of experiment.

### *Histological Study*

Rats were euthanized by dislocation of cervical vertebrae. Bone cutter was used to open the skull and half of cerebral specimens were fixed in 10% formol saline for paraffin blocks preparation. Sections were stained with:

1. Hematoxylin & Eosin (H&E) stain[19]
2. Congo red stain (CR)[20] to detect β-amyloid (Aβ) substance, the main pathological hallmark of AD.
3. Perls Prussian blue stain (Pb)[21]
4. Caspase3[22] immunostaining, the marker for apoptosis. A rabbit monoclonal antibody (700182, 9H19L2), (Lab Vision Corporation, USA).
5. Glial fibrillary acidic protein (GFAP) immunostaining, the marker for astrocytes[23]. It A rabbit monoclonal antibody, (MS-1376-PO) (Lab Vision Corporation, USA).

### *Morphometric Study*

Image analyizer (500 LTD, Leica Qwin Corporation, Cambridge, UK), was used to determine area of atypical neurons and CR +ve neurons in 10 non overlapping fields x200. Area % of Caspase 3 and GFAP positive immunoexpression (IE) were assessed by binary menu x200.

### *Fluorescent Microscopic Study*

Sections were placed in Xylol and photographed by fluorescent microscope. GFP labeled sections[14].

Quantitative polymerase chain reaction (qPCR) for gene (SERCA2b) preparation and assessment

Reverse Transcription was carried out using paraffin sections. The SERCA2b gene specific primer was, (forward primer: 5′ AAGTGCAATACCTCACTCG 3′, reverse primer: 5′ GATCAGCAGCAGACATATC 3′) [10]. By using RNA, the complementary DNA strand was formed for gene preparation. SERCA2b gene was quantitated on PCR program.

### *Western blot (Wb) analysis*

SERCA2b and Beta amyloid protein contents were assessed and normalized to actin[24].

### *Biochemical study*

The other half of cerebral specimens was freezed for homogenization. 1 gram of each cerebral homogenate (Ortoalresa, Spain) was centrifuged. Colorimetric method kits were provided by (Biodiagnostic, Egypt) to assess:

- Cerebral $Ca^{2+}$ concentration[25]
- Malondialdehyde (MDA)[26] and catalase[27]

### *Statistical Study*

Analysis was done using ANOVA test and *P-values* <0.05 were proved to be sig. Statistical Package for the Social Sciences (SPSS) version (16) was used.

## RESULTS

Reduced activity and increased urine output were notified in rats diagnosed to be positive for diabetes, these observations regressed in animals that received treatment. Two animals belonging to the diabetic group passed out at start of present work, two days following STZ injection and were compensated.

### *Immunophenotyping of Adipose mesenchymal SCs and modified Adipose mesenchymal SCs*

Positive immunoexpression was visualized with CD105, CD34 showed no expression. Percentage determined by FC was 96.9 %. GFP tagged modified AMSCs were spindle. And % was 95.8 % (Figure 1).

### *Neurological and behavioral Results*

Mean values of alternation score (%) in Y -Maze test expressed sig reduction in group B, in group C versus groups A and D. Open field test expressed a sig decrease in group D versus group A, in addition (Table 1a).

### *Serum Glucose Values*

Sig elevation was found in group B, in group C versus groups A and D, in group D versus group A (Table 1a).

### *Histological phenotyping*

Group A, revealed molecular, external granular, external pyramidal (EP), internal granular, internal pyramidal, pleiomorphic layers of cerebral cortex (Figure 2a). Sections in the EP layer of cerebral cortex demonstrated multiple pyramidal neurons exhibiting large round vesicular nuclei and scanty cytoplasm with well-defined main dendrite. Granule cells and stellate neurons were also seen in EP layer. Microglia have elongated darkly stained and astrocytes have pale nuclei (Figure 2b). Sections in dentate gyrus (DG) of hippocampus recruited dentate molecular layer (DML), granular (GL) and dentate polymorphic (DOL) layers. Granular layer contains crowded nerve cells each exhibiting a pale nucleus. The DML as well as DOL demonstrated scanty scattered nerve cells as well as neuroglia in neuropil (Figure 2c). Group B showed some fields of EP layer exhibiting multiple pyramidal neurons with acidophilic cytoplasm containing disintegrated nuclei. Deformed neurons with acidophilic cytoplasm were detected, while others were deformed and having dark nuclei (Figure 2d). DG exhibited multiple neurons in GL with dark nuclei, neuropil vacuolations, acidophilic masses with a vacuolated area around and many microglia (Figure 2e).

Group C demonstrated some atypical nerve cells with acidophilic cytoplasm and apoptotic nuclei with vacuolated area around, many apparently normal pyramidal, stellate

and granule nerve cells in EP layer (Figure 3a). Dentate gyrus exhibited closely arranged neurons with vesicular nuclei in the GL, some deformed neurons with darkly-stained nuclei, neuropil vacuolations, some microglia and few astrocytes (Figure 3b). In group D, EP layer exhibited multiple apparently normal pyramidal neurons with well-defined main dendrite, stellate and granule neurons, few deformed neurons with acidophilic cytoplasm and with vacuolated area around, scanty microglia as well as astrocytes (Figure 3c). Dentate gyrus recruited pale nuclei in multiple crowded arranged nerve cells, accidental neurons with dark nuclei among localized neuropil vacuolations and accidental small acidophilic masses (Figure 3d).

In Congo red (CR) stained sections, EP layer and DG of group A showed pale appearance of nerve cells and neuropil (Figures 4 a,b). Strongly +ve deposits were found in multiple neurons of EP layer, among neurons as well as neuropil of DG of group B (Figures 4 c,d). Group C revealed strongly positive deposits in few neurons of EP layer and fewer and smaller strongly +ve deposits among neurons of DG (Figures 4 e,f). Group D showed minimal strongly +ve deposits in few neurons of EP layer and few small strongly +ve deposits among neurons of DG (Figures 4 g,h).

The EP layer and the DG exhibited -ve Caspase3 immunoexpression (IE) in group A (Figures 5 a,b), +ve IE in multiple neurons (Figures 5 c,d) in group B. On contrary, group C, showed fewer neurons with +ve IE (Figures 5 e,f) and, +ve IE in few neurons (Figures 5 g,h) in Group D. In GFAP immunoexpression (IE), in group A, EP layer and DG exhibited +ve IE in few astrocytes among neurons (Figures 6 a,b). In group B, +ve IE was found in multiple astrocytes (Figures 6 c,d). On contrary, group C recruited +ve IE of fewer astrocytes (Figures 6 e,f). In group D, +ve IE was noticed in few astrocytes (Figures 6 g,h).

### *Morphometric results (Table 1b)*

Area of atypical nerve cells, CR+ve neurons as well as area% of caspase3 +ve and GFAP +ve IE indicated sig increase in diabetic versus treated rats as well as AMSCs treated rats versus AMSCs gene modified treated rats.

### *Tracking AMSCs and transfected AMSCs*

Many Pb tagged AMSCs were detected in EP layer, attached to neurons, in the lumen of vessels as well as among neuropil in group C. DG demonstrated Pb stained cells among neurons, inside blood vessels and among the neuropil. (Figures 7 a,b). In group D, multiple GFP labeled cells were detected mainly in EP layer of cerebral cortex and DG of hippocampus (Figures 7 c,d).

### *PCR results*

The mean SERCA2b gene values in μg in groups A, B, C and D were (1.56±0.19), (0.32±0.04), (0.76±0.15) and (1.51±0.21) respectively, expressing sig decrease ($P < 0.05$) in group B versus groups A, C as well as D, in group C versus groups A as well as D (Figure 7e).

### *Values of Wb*

The mean values of SERCA2b protein in control, diabetic and AMSCs and gene modified AMSCs treated rats were (2.38±0.18), (0.46± 0.07), (1.38± 0.15) and (2.25± 0.39), denoting a sig decrease ($P < 0.05$) in diabetic rats versus control and treated rats, in AMSCs treated rats versus control as well as AMSCs gene modified treated rats (Figure 7f). Beta amyloid protein levels in control, diabetic and AMSCs and gene modified AMSCs treated rats were (1.05± 0.09), (4.76± 0.29), (2.19± 0.13) as well as (1.65± 0.31) respectively, expressing a sig increase ($P < 0.05$) in diabetic rats versus other rats, in AMSCs treated rats versus control as well as AMSCs gene modified treated rats, in latter group versus control (Figure 7g).

### *Biochemical Data*

Calcium ion concentration was reported as (8.56± 0.66), (7.13± 0.10), (7.47± 0.16) and (8.33± 0.60) for control, diabetic and treated rats respectively, indicating sig reduction in diabetic rats as well as AMSCs treated rats versus control as well as AMSCs gene modified treated rats. The mean values of MDA expressed (40±2.11), (136.91± 7.03), (83.44 ±0.70) and (58.31±2.66) for groups A, B, C and D respectively, denoting a sig increase in diabetic rats versus all rats, in AMSCs treated rats versus control as well as AMSCs gene modified treated rats, in the latter rats versus control. The mean values of catalase were (213.69 ±2.13), (103.25 ±1.56), (193.51±6.14) and (208.10±1.70) respectively, confirming a sig decrease in diabetic rats versus all rats, in AMSCs treated rats versus control as well as AMSCs gene modified treated rats, in the latter rats versus control (Figure 7h).

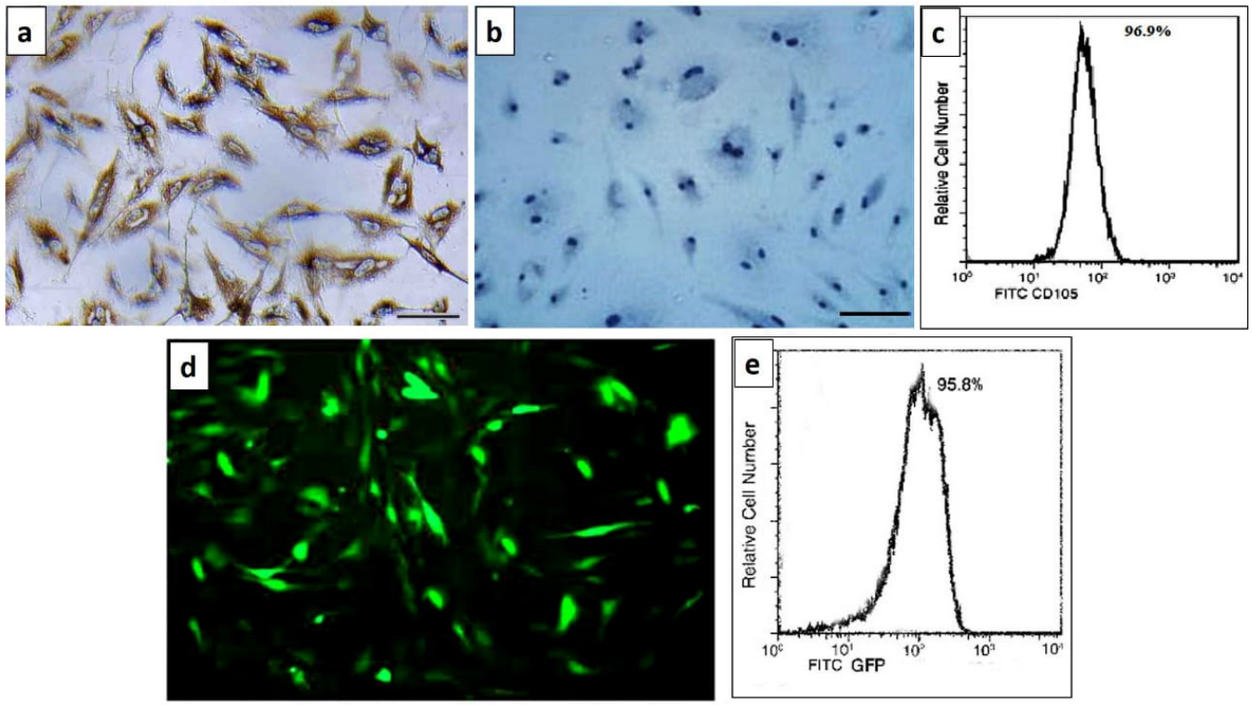


**Fig. 1 showing:** (a) CD105 +ve spindle cells (b) CD34 –ve IE (a and b: Phase contrast microscopy x 400 and 100 respectively). (c) 96.9 % CD105 +ve cells (Flow Cytometry). (d) GFP tagged modified AMSCs were spindle (GFP x100) (e) 95.8% GFP labeled cells (Flow Cytometry).

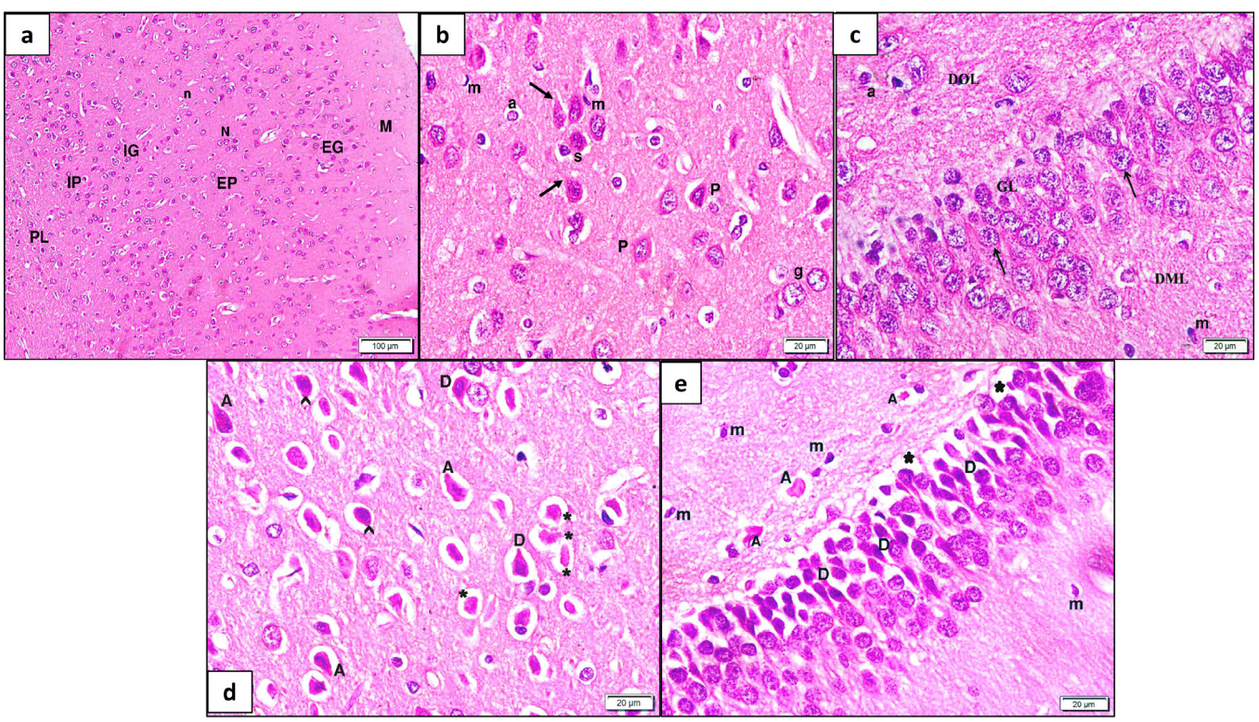


**Fig. 2 showing:** In group A: (a) molecular (M), external granular (EG), external pyramidal (EP), internal granular (IG), internal pyramidal (IP), pleiomorphic (PL) layers of cerebral cortex (H&E, x100) (b) multiple apparently normal pyramidal (P) with well-defined main dendrites (arrows), granule (g) and stellate (s) neurons, microglia (m) and astrocytes (a) in EP layer. (c) DML, GL, DOL, pale nuclei (arrows) of GL neurons, few microglia (m) and astrocytes (a) in DML and DOL. In group B: (d) multiple pyramidal neurons with acidophilic cytoplasm and disintegrated nucleus (A), deformed neurons with acidophilic cytoplasm (*), deformed and having dark nuclei (^) in EP layer. (e) DG exhibited multiple neurons in GL with dark nuclei (D), neuropil vacuolations (*), acidophilic masses (A) and many microglia (m). (H&E, x400)

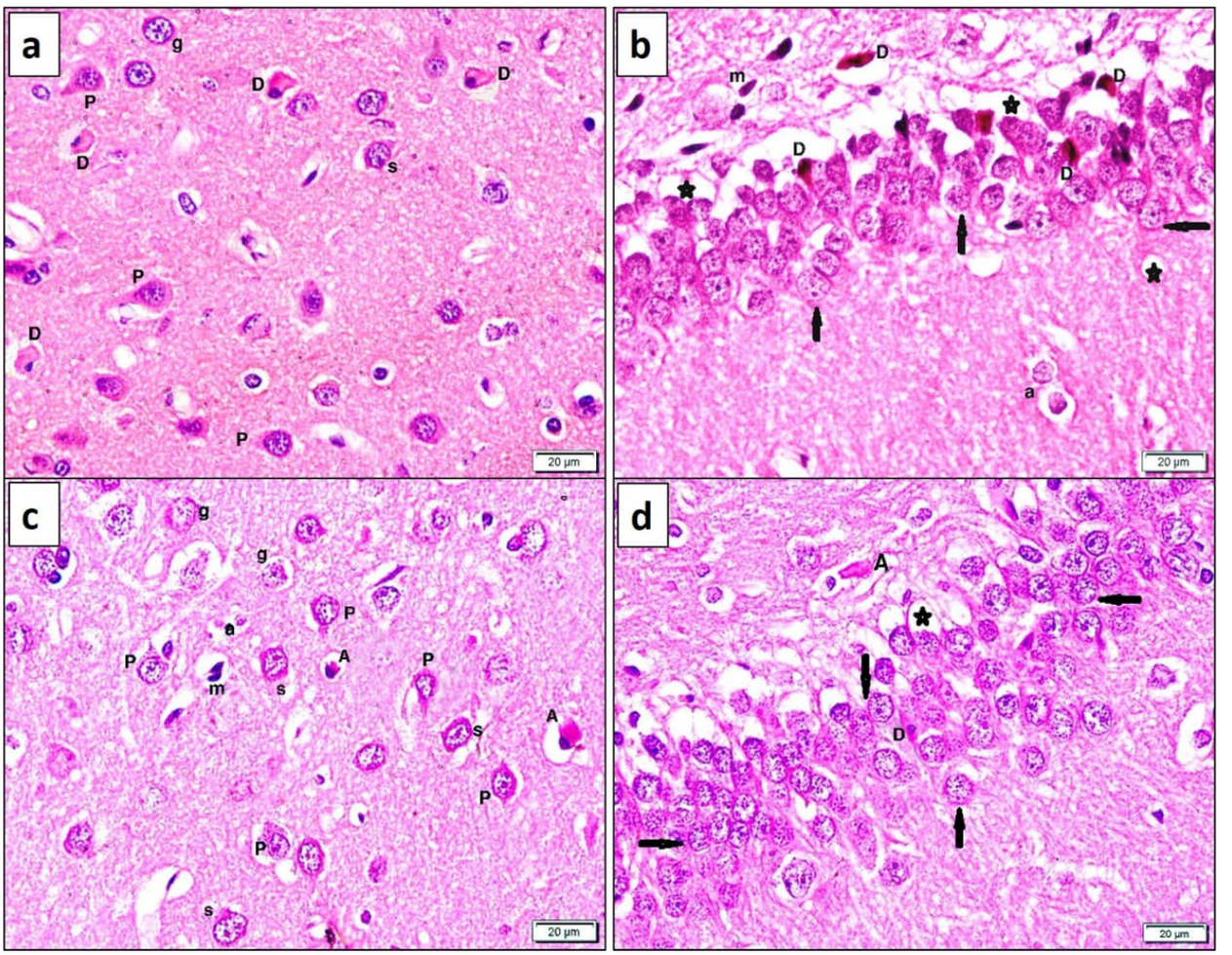


**Fig. 3 showing:** (a) In group C: some atypical nerve cells with acidophilic cytoplasm and apoptotic nuclei (D), multiple pyramidal (P), stellate (s) and granule (g) neurons in EP layer. (b) In group C: neurons with vesicular nuclei (arrows), some deformed neurons with darkly-stained nuclei (D), neuropil vacuolations (*), some microglia (m) and few astrocytes (a) in DG. (c) In group D: few deformed neurons with acidophilic cytoplasm (A), multiple pyramidal (P), stellate (s) and granule (g) neurons, scanty microglia (m) and astrocytes (a) in EP layer. (d) In group D: neurons with pale nuclei (arrows), a deformed neuron with dark nucleus (D), localized neuropil vacuolations (*) and a small acidophilic mass (A). (H&E, x400)

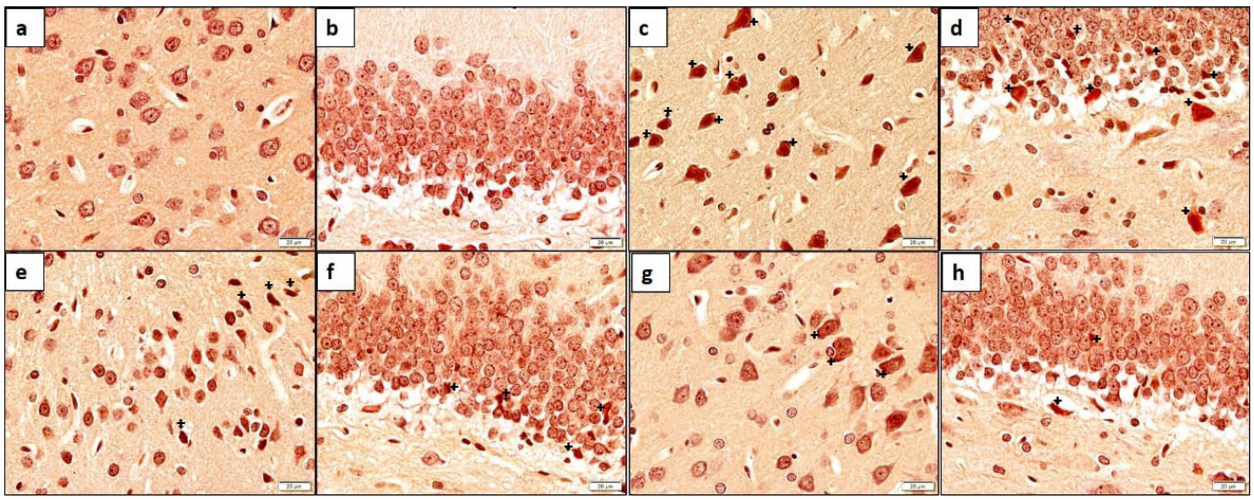


**Fig. 4 showing:** In Group A: pale appearance of nerve cells and neuropil in (a) EP layer and (b) DG. (c) In group B: Strongly +ve deposits in multiple neurons (+) of EP layer. (d) In group B: multiple strongly +ve small and large deposits among neurons (+) of DG. (e) In group C: strongly +ve deposits in few neurons (+) of EP layer. (f) In group C: fewer and smaller strongly +ve deposits among neurons (+) of DG. (g) In group D: minimal strongly +ve deposits in few neurons (+) of EP layer. (h) In group D: few small strongly +ve deposits among neurons (+) of DG. (CR, x400)

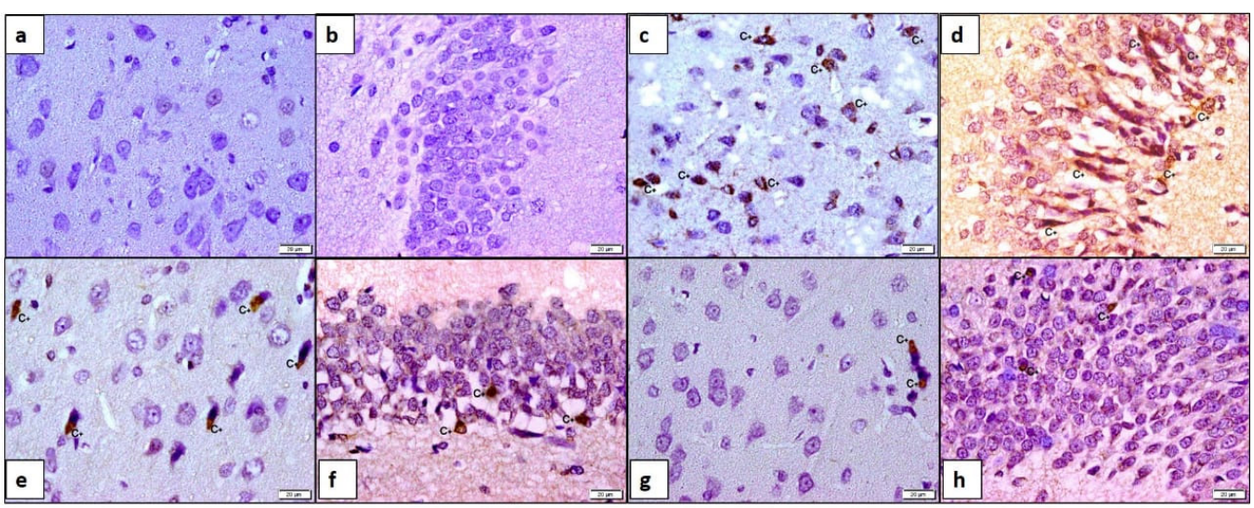


**Fig. 5 showing:** Caspase3 immunoexpression in group A: -ve in (a) EP layer and (b) DG. In group B: +ve (C+) in multiple neurons in (c) EP layer and (d) DG. In group C: +ve (C+) in fewer neurons in (e) EP layer and (f) DG. In group D: +ve (C+) in few neurons in (g) EP layer and (h) DG. (Caspase3 immunostaining, x400)

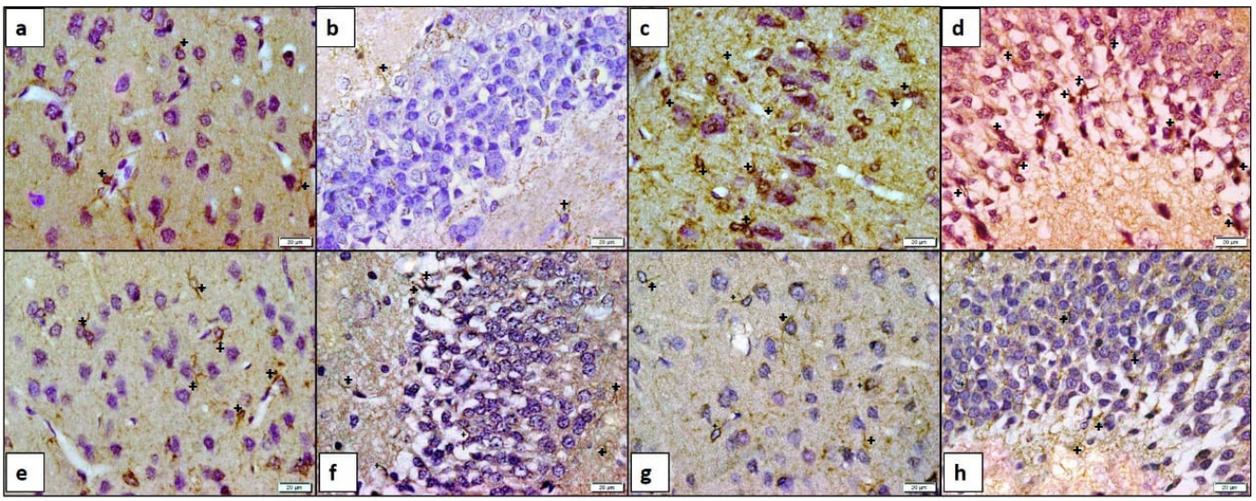


**Fig. 6 showing:** GFAP immunoexpression in group A: +ve (+) in few astrocytes among neurons in (a) EP layer and (b) DG. In group B: +ve (+) in multiple astrocytes in (c) EP layer and (d) DG. In group C: +ve (+) in fewer astrocytes in (e) EP layer and (f) DG. In group D: +ve (+) in few astrocytes in (g) EP layer and in (h) DG. (GFAP immunostaining, x400)

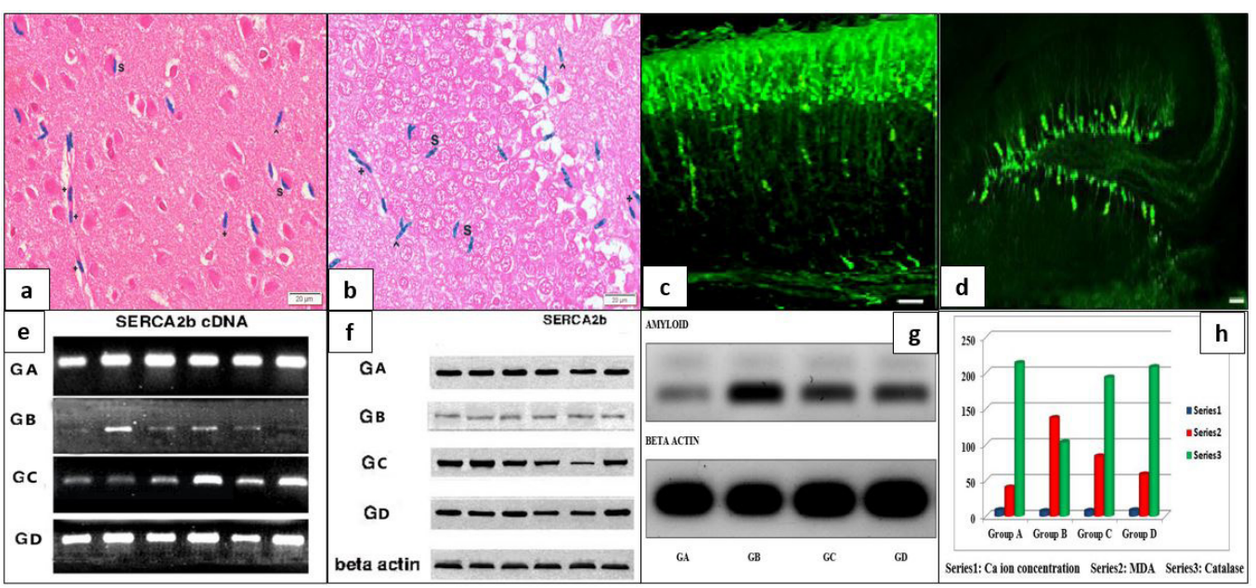


**Fig. 7 showing:** (a) In group C: Many Pb tagged AMSCs attached to neurons (s), in the lumen of vessels (+) as well as among neuropil (^) in EP layer. (b) In group C: multiple Pb stained spindle cells among neurons (s), inside blood vessels (+) and among neuropil (^) in DG. (Pb, x400). In group D: multiple GFP labeled cells mainly in (c) EP layer and (d) DG (GFP, x100). (e) qPCR of SERCA2b gene. (f) Wb of SERCA2b protein normalized to actin. (g) Wb of beta amyloid protein normalized to actin. (h) histogram of $Ca^{2+}$ concentration, MDA and catalase values.

**Table 1a:** Mean values (±standard deviation (SD)) of neurological tests (Y -Maze and open field) and blood glucose level

| | | Group A | Group B | Group C | Group D |
|---|---|---|---|---|---|
| Y -Maze test (Alternation score (%)) | | 88.67 ± 4.89 | 55.88 ± 4.51■ | 67.06 ± 9.46● | 79.85 ± 9.71 |
| Open field test | Number of line crossing | 151.75 ± 6.22 | 50.25 ± 1.48■ | 79 ± 5.12● | 103.62 ± 10.07^ |
| | Number of center square entries | 13.25 ± 1.28 | 1.37± 0.51■ | 3.62 ± 0.74● | 7.87 ± 1.45^ |
| | Center square duration (sec) | 41.75 ± 2.60 | 8.25 ± 1.90■ | 15.50 ± 1.41● | 25.75 ± 4.55^ |
| | Rearing frequency | 48 ± 4.50 | 14.75 ± 5.67■ | 22.75 ± 3.61● | 37.62 ± 3.02^ |
| | Blood glucose level | 98.23 mg/dl ±0.78 | 440.17 mg/dl ±3.40* | 155.31 mg/dl ± 2.79 # | 128.03 mg/dl ± 1.43♦ |

Sig ($P$<0.05)

■ Decrease compared to control and treated groups.

● Decrease compared to control and group D.

^ Decrease compared to control group.

* Increase compared to control and treated groups.

# Increase compared to control and group D.

♦ Increase compared to control group.

**Table 1b:** The mean area of deformed neurons, CR+ve neurons and mean area% of caspase3 +ve and GFAP +ve IE ± SD

| Groups | Area of atypical neurons | Area of CR+ve neurons | Area% of caspase3 +ve IE | Area% of GFAP +ve IE |
|---|---|---|---|---|
| Group A | 0 | 0 | 0 | 0.21 ± 0.02 |
| Group B | 40.09 ± 12.74* | 65.80 ± 8.44* | 8.40 ± 2.05* | 3.77 ± 0.49* |
| Group C | 29.72 ± 4.70^ | 35.03 ± 6.43^ | 2.79 ± 0.53^ | 0.69 ± 0.15^ |
| Group D | 15.84 ± 4.67 | 11.11 ± 2.35 | 0.17 ± 0.02 | 0.26 ± 0.04 |

sig ($P$<0.05)

* increase versus groups C and D ^ increase versus group D

## DISCUSSION

Clinical research and animal experiment proved that encephalopathy complicating T1DM is similar to brain ageing developing in neurodegenerative diseases. AD being the most common one, is characterized by memory loss and other intellectual disabilities due to impact on the cerebral cortex and hippocampus. Rats and mice models were proved to develop neurodegenerative changes simulating those in human brain of AD[28]. Induction of T1DM was performed by injection of STZ, that induces fast and irreversible necrosis due to selective destruction of β-cells of islets of Langerhans in rats[1]. Prevalence and severity of AD was documented in women more than men, similarly, in female rats. This can be related to sex steroid hormones, antioxidant defense system and neurotransmitters[29].

The diabetic rats expressed reduced neurological and behavioral values, in AMSCs treated rats versus control as well as AMSCs gene modified treated rats, confirming neuronal degeneration and dysfunction, that improvement particularly by SERCA gene therapy. In support, cholinergic neuronal cell death and dysfunction develops due to amyloid-β plaques deposition prefrontal cortical area as well as dentate gyrus. Latter regions determine memory for space, which when disabled represent main characteristic features of AD[19].

Stem cells were reported to secrete brain-derived neurotrophic growth factor, promote angiogenesis and improve blood flow[30], consequently repairing cognitive dysfunction. In addition, it was confirmed that calcium regulated by SERCA2b in mammalian neurons is essential for neuronal development, neurotransmitter release and signal transduction. Using SERCA gene, considered a recent treatment modality, either by stimulation using SERCA activators or through controlling SERCA expression by genetic manipulations[31].

The blood glucose level revealed sig increase in diabetic rats, in AMSCs treated rats versus control as well as AMSCs gene modified treated rats, in the latter rats versus control, which proved blood group tests sensitivity. In support, the hyperglycemic lowering effect of MSCs can be referred to regenerating pancreatic islets and beta cells that produce insulin[32]. In addition, insulin secretion is a $Ca^{2+}$ dependent process, $Ca^{2+}$ ions being stored in endoplasmic reticulum controlled by SERCA protein expressed by the gene, exerting homeostasis[33].

Group B recruited EP layer exhibiting multiple atypical neurons with acidophilic cytoplasm and disintegrated or dark nuclei, multiple microglia and astrocytes. DG showed obvious neuropil vacuolations and few acidophilic masses, in addition. The increased area of atypical neurons was

confirmative versus treated groups, denoting degenerative changes. In accordance, Luebke *et al*[34] focused specifically on layer III (EP) pyramidal neurons because they are the principal neurons responsible for high intellectual activities affected in neurodegeneration. Recently, Ali *et al*[35] confirmed that pyknotic nuclei were found in neurons of cerebral cortex and hippocampus of AD rat model.

In support, it was pointed to vacuolated neuropil in DG and neuronal degeneration in EP layer of prefrontal cortex[19]. Bashir *et al*[22] added that pyramidal cells of cerebral cortex showed chromatolysis and karyolitic nuclei. In the hippocampus, the pyramidal cells showed dystrophic changes and spongiform vacuoles in the neuropils. Apoptosis of nerve cells were found to be intimately related to ROS accumulation. In agree, AD was proved to stimulate microglial proliferation and phagocytic activities, the latter become insufficient with progress of the disease. Activated microglia may activate astrocytes, that stimulate inflammation[36].

Group C showed EP layer exhibiting fewer deformed neurons. DG exhibited localized vacuolations in neuropil, fewer microglia and few astrocytes, in addition. Significantly increased atypical neurons' area was noted versus gene modified AMSCS treated rats. In agreement with, administrated MSCs to AD animal models were recorded to move to the brain and enhance neurogenesis, neuronal differentiation, endogenous neural precursor cells and signaling actions, modulating brain homeostasis[37].

Group D revealed few deformed neurons, few microglia and astrocytes. The DG contained localized vacuolations and accidental small masses. It can be commented that, decreased microglia accompany less abundant necrotic cells. In support, AD proved misbalance of intracellular calcium concentration that initiate neurodegeneration. Delivery of therapeutic gene into the cell restores histophysiology[38].

Significantly increased CR+ve area was found in group B, in comparison to treated groups. Concomitantly, extracellular aggregation of Aβ as CR +ve plaques appeared in cortex and hippocampus, indicating neuroinflammation followed by degeneration and memory impairment in AD mice model [20].

Significantly increased area of CR+ve neurons was detected in group C versus group D, which showed minimal strongly +ve deposits. It can be proposed that transplanted MSCs were proved to exert anti-inflammatory and antioxidant actions. In support, unfolded protein such as amyloid and tau in AD that lead to endoplasmic reticulum (ER) stress. SERCA was proved to decrease ER stress by controlling $Ca^{2+}$ homeostasis, consequently improves memory function and cognition[39].

Significantly increased area% of caspase3 and glial fibrillary acidic protein IE was found in diabetic rats versus treated rats and in AMSCs treated rats gene modified AMSCs treated rats. In support, caspase-3 was confirmed to be significantly activated in neuronal degeneration and represents a measure for neuronal apoptosis caused by oxidative stress[22]. It was added that astrogliosis is associated with elevated Aβ aggravation and neuronal death[23]. Transplanted MSCs were proved to exert repeated division and differentiation abilities[40], while SERCA overexpression inhibits neuronal apoptosis by restoring $Ca^{2+}$ homeostasis that blocks the Aβ-induced astrogliosis[41].

Multiple Pb stained spindle cells were found attached to neurons of EP layer and among neurons of DG, inside blood vessels and among neuropil in group C. Group D showed multiple GFP labeled cells in EP layer and DG. In accordance, ferrumoxide tagging of SCs, to be stained with Pb was proved not to affect SCs viability[21]. GFP is used as a marker for co-localization of transfected SCs, namely lipofectamine 3000 transfection[17].

The mean SERCA2b gene and protein values expressed decrease in diabetic rats, in AMSCs treated rats versus control as well as gene transfected AMSCs treated rats. It can be concluded, that impaired SERCA including SERCA2b function leads to increased intracellular calcium concentration and triggers ER stress that is associated with neurodegenerative diseases and diabetes. Recently, it was reported that the efficacies of MSCs on chronic diseases, is by decreasing ER stress, rescuing SERCA gene via regenerative plasticity[41]. Similarly, mRNA was used to form SERCA2b gene and quantitation by RT-qPCR. In addition the levels of SERCA2b protein detected by Western blotting, revealed significant increase in SERCA2b protein in cocultured MSCs[42].

While, the mean beta amyloid protein proved a sig increase in diabetic rats, in AMSCs treated rats versus control as well as gene transfected AMSCs treated rats, the latter rats versus control, expressing sensitivity of quantitation of Aβ protein. It was added that Wb recorded age-related agreggation of amyloid beta protein within cerebrum in AD[24]. Zhang *et al*[43] proved that MSCs can eliminate Aβ by inducing secretion of Aβ proteolytic enzymes in microglia and can regulate cell autophagy. Xu and Van Remmen[31] commented that changes in homeostasis of ER $Ca^{2+}$ pool is a key point in regulation of Aβ production. Activation of SERCA resumes $Ca^{2+}$ homeostasis, consequently reduces Aβ accumulation.

Values of mean Ca ion concentration reported a sig decrease in diabetic rats, in AMSCs treated rats versus control as well as gene transfected AMSCs treated rats. This can be due to decreased SERCA expression keeping Ca ion homeostasis. Concomitantly, it was confirmed that in diabetes, disrupted calcium storage in neuronal ER was recorded. It was added that neurons from diabetic animals displayed lower ER $Ca^{2+}$ content, and reduced $Ca^{2+}$ uptake into the ER[25]. MSCs were found to modulate $Ca^{2+}$ by relieving ER stress[41], consequently downregulating calcium in the cytoplasm. SERCA gene therapy helps

pumping $Ca^{2+}$ from the cytoplasm into the ER, which maintain the $Ca^{2+}$ dynamics in the cytosol and fills up the ER lumen with high $Ca^{2+}$ levels[39].

Values of mean MDA and catalase expressed a sig increase and decrease respectively in diabetic rats, in AMSCs treated rats versus control as well as gene transfected AMSCs treated rats, in the latter rats versus control. The biochemical results reflected disruption of oxidant- antioxidant enzyme system in the diabetic group. Restoration of the balance of the system was proved by MSCs injection and more obviously by SERCA gene therapy.

In support to the previous findings, oxidative imbalance is a crucial factor inducing AD. Due to the brain's high oxygen demand, oxidative stress affects it the most. ROS are highly produced in hippocampus and frontal cortex of AD patients, which causes brain damage. Lipid peroxidation and karyorrhexis of DNA during apoptosis develop 2ry to ROS production. Malondialdehyde is considered a degradation product that determines value of lipid peroxidation[26]. One of the main protective systems against oxidative damage is catalase, interrupting neurotransmission[27].

It was mentioned that MSCs ameliorate oxidant damage and activate catalase synthesis[44]. It was documented that SERCA, is crucial for keeping Ca ion homeostasis participated between ER and cytosol. Consequently, regaining neuronal integrity affected in neurodegeneration[45].

## CONCLUSION

In conclusion, TIDM precipitated morphological findings denoting neurodegeneration in the cerebrum and hippocampus in a model of rat for AD. Amelioration of degenerative structural changes in response to adipose derived MSCs and SERCA2b gene transfected adipose derived MSCs was confirmed. Stem cells transfected with sarcoplasmic reticulum calcium ATPase2b gene proved pronounced therapeutic impact suggesting its potency and regenerative capacity in remarkable amelioration of Alzheimer's disease complicating diabetes I. Neurological, serological, morphometric, qPCR, WB as well as biochemical parameters proved the concluded findings.

## CONFLICT OF INTERESTS

There are no conflicts of interest.

## REFERENCES


1. Pardeshi R, Bolshette N, Gadhave K, Arfeen M, Ahmed S, Jamwal R, Hammock BD, Lahkar M and Goswami SK (2019): Docosahexaenoic acid increases the potency of soluble epoxide hydrolase inhibitor in alleviating streptozotocin-induced alzheimer's disease-like complications of diabetes. Front Pharmacol. DOI: 10:288-301. 10.3389/fphar.2019.00288.
2. Yu F, Han W, Zhan G, Li S, Xiang S, Zhu B, Jiang X, Yang L, Luo A, Hua F and Yang C (2019): Abnormal gut microbiota composition contributes to cognitive dysfunction in streptozotocin-induced diabetic mice. AGING, 11(10): 3262- 3279. DOI: 10.18632/aging.101978.
3. Prestia FA, Galeano P, Adami PV, Do Carmo S, Castaño EM, Cuello AC and Morelli L (2019): Platelets bioenergetics screening reflects the impact of brain aβ plaque accumulation in a rat model of Alzheimer. Neurochem Res, 44(6): 1375-1386. DOI: 10.1007/s11064-018-2657-x.
4. Cao J, Hou J, Ping J and Cai D (2018): Advances in developing novel therapeutic strategies for Alzheimer's disease. Mol Neurodegener, 13(1): 64-84. DOI: 10.1186/s13024-018-0299-8.
5. Ferreira AC, Sousa N, Bessa JM, Sousa JC and Marques F (2018): Metabolism and adult neurogenesis: towards an understanding of the role of lipocalin-2 and iron-related oxidative stress. Neurosci Biobehav Rev, 95: 73-84. DOI: 10.1016/j.neubiorev.2018.09.014.
6. Klemenz AC, Meyer J, Ekat K, Bartels J, Traxler S, Schubert JK, Kamp G, Miekisch W and Peters K (2019): Differences in the emission of volatile organic compounds (vocs) between non-differentiating and adipogenically differentiating mesenchymal stromal/stem cells from human adipose tissue. Cells, 8(7): 697-711. DOI: 10.3390/cells8070697.
7. Ijomone OM, Aluko OM, Okoh CO, Martins AC and Aschner M (2019): Role for calcium signaling in manganese neurotoxicity. J Trace Elem Med Biol, 56: 146-155. DOI: 10.1016/j.jtemb.2019.08.006.
8. Shomali N, Gharibi T, Vahedi G, Mohammed R, Mohammadi H, Salimifard S and Marofi F (2019): Mesenchymal stem cells as carrier of the therapeutic agent in the gene therapy of blood disorders. J Cell Physiol, 235(5): 4120-4134. DOI: 10.1002/jcp.29324.
9. Britzolaki A, Saurine J, Klocke B and Pitychoutis PM (2020): A role for serca pumps in the neurobiology of neuropsychiatric and neurodegenerative disorders. Adv Exp Med Biol, 1131: 131-161. DOI: 10.1007/978-3-030-12457-1_6.
10. Prasad V, Lorenz JN, Lasko VM, Nieman ML, Huang W, Wang Y, Wieczorek DW and Shull GE (2015): SERCA2 Haploinsufficiency in a Mouse Model of Darier Disease Causes a Selective Predisposition to Heart Failure. Biomed Res Int, 2015: 251598-251619. DOI: 10.1155/2015/251598.
11. Zickri MB, Aboul-Fotouh GI, Omar AI, El-Shafei AA and Reda AM (2018): Effect of stem cells and gene transfected stem cells therapy on the pancreas of experimentally induced type 1 diabetes. Int J Stem Cells, 11(2): 205-215. DOI: 10.15283/ijsc18002.

12. Abdel Halim AS, Ahmed HH, Aglan HA, Abdel Hamid FF and Mohamed MR (2021): Role of bone marrow-derived mesenchymal stem cells in alleviating pulmonary epithelium damage and extracellular matrix remodeling in a rat model of lung fibrosis induced by amiodarone. Biotech Histochem, 96(6): 418-430. DOI: 10.1080/10520295.2020.1814966

13. Zhang Y, Jiang X and Ren L (2019): Optimization of the adipose derived mesenchymal stem cell delivery time for radiation-induced lung fibrosis treatment in rats. Sci Rep, 9(1): 5589-5598. DOI: 10.1038/s41598-019-41576-5.

14. Tang X, Chen F, Lin Q, You Y, Ke J, Zhao S (2017): Bone marrow mesenchymal stem cells repair the hippocampal neurons and increase the expression of IGF-1 after cardiac arrest in rats. Exp Ther Med, 14(5): 4312-4320. DOI: 10.3892/etm.2017.5059.

15. Rezapour-Lactoee A, Yeganeh H, Gharibi R and Milan PB (2020): Enhanced healing of a full-thickness wound by a thermoresponsive dressing utilized for simultaneous transfer and protection of adipose-derived mesenchymal stem cells sheet. J Mater Sci Mater Med, 31(11): 101-113. DOI: 10.1007/s10856-020-06433-2.

16. Abouelnaga H, El-Khateeb D, Moemen Y, El-Fert A, Elgazzar M and Khalil A (2022): Characterization of mesenchymal stem cells isolated from Wharton's jelly of the human umbilical cord. Egypt Liver J, 12: 28-36. DOI: 10.1007/s10856-020-06433-2.

17. Thongbamrer C, Roobsoong W, Sattabongkot J, Opanasopit P and Yingyongnarongkul BE (2022): Serum Compatible Spermine-Based Cationic Lipids with Nonidentical Hydrocarbon Tails Mediate High Transfection Efficiency. Chembiochem, 23(6): e202100672-202100682. DOI: 10.1002/cbic.202100672.

18. Galeano P, Adami PM, Carmo SD, Blanco E, Rotondaro C, Capani F, Castaño EM, Cuello AC and Morelli L (2014): Longitudinal analysis of the behavioral phenotype in anovel transgenic rat model of early stages of Alzheimer's disease. Front Behav Neurosc, 8: 321-335. DOI: 10.3389/fnbeh.2014.00321.

19. Mandour DA, Bendary MA and Alsemeh AE (2021): Histological and imunohistochemical alterations of hippocampus and prefrontal cortex in a rat model of Alzheimer like-disease with a preferential role of the flavonoid "hesperidin". J Mol Histol, 52(5):1043-1065. DOI: 10.1007/s10735-021-09998-6.

20. Liu X, Zhou Q, Zhang JH, Wang KY, Saito T, Saido TC, Wang X, Gao X and Azuma K (2021): Microglia-Based Sex-Biased Neuropathology in Early-Stage Alzheimer's Disease Model Mice and the Potential Pharmacologic Efficacy of Dioscin. Cells, 10(11): 3261-3280. DOI: 10.3390/cells10113261.

21. Qadri Z, Righi V, Li S and Tzika AA (2021): Tracking of Labelled Stem Cells Using Molecular MR Imaging in a Mouse Burn Model in *Vivo* as an Approach to Regenerative Medicine. Adv J Mol Imaging, 11(1): 1-15. DOI: 10.4236/ami.2021.111001.

22. Bashir DW, Rashad MM, Ahmed YH, Drweesh EA, Elzahany EAM, Abou-El-Sherbini KS and El-Leithy EMM (2021): The ameliorative effect of nanoselenium on histopathological and biochemical alterations induced by melamine toxicity on the brain of adult male albino rats. Neurotoxicology, 86: 37-51. DOI: 10.1016/j.neuro.2021.06.006.

23. Jurga AM, Paleczna M, Kadluczka J and Kuter KZ (2021): Beyond the GFAP-Astrocyte Protein Markers in the Brain. Biomolecules, 11(9):1361-1388. DOI: 10.3390/biom11091361.

24. Bugrova AE, Strelnikova PA, Indeykina MI, Kononikhin AS, Zakharova NV, Brzhozovskiy AG, Barykin EP, Pekov SI, Gavrish MS, Babaev AA, Kosyreva AA, Morozova AA, Degterev DA, Mitkevich VA, Popov IA, Makarov AA and Nikolaev EN (2022): The Dynamics of β-Amyloid Proteoforms Accumulation in the Brain of a 5xFAD Mouse Model of Alzheimer's Disease. Int. J. Mol. Sci, 23(1): 27-41. DOI: 10.3390/ijms23010027.

25. Kasozi KI, Nakimbugwe D, Ninsiima HI, Kasolo J, Matama K, Safiriyu AA, Owembabazi E, Ssempijja F, Okpanachi AO and Valladares MB (2021): Calcium and s100a1 protein balance in the brain-heart axis in diabetic male Wistar rats. J Basic Clin Physiol Pharmacol, 32(1): 20200074-20200081. DOI: 10.1515/jbcpp-2020-0074.

26. Xiang X, Wang X, Jin S, Hu J, Wu Y, Li Y and Wu X (2022): Activation of GPR55 attenuates cognitive impairment and neurotoxicity in a mouse model of Alzheimer's disease induced by Aβ1-42 through inhibiting RhoA/ROCK2 pathway. Prog Neuropsychopharmacol Biol Psychiatry, 112: 110423-110432. DOI: 10.1016/j.pnpbp.2021.110423.

27. Vahdati SN, Lashkari A, Navasatli SA, Ardestani SK and Safavi M (2022): Butylated hydroxyl-toluene, 2,4-Di-tert-butylphenol, and phytol of Chlorella sp. protect the PC12 cell line against H2O2-induced neurotoxicity. Biomed Pharmacother, 145: 112415-112427. DOI: 10.1016/j.biopha.2021.112415.

28. Zhang YM, Zheng T, Huang TT, Gu PP, Gou LS, Ma TF and Liu YW (2021): Sarsasapogenin attenuates Alzheimer-like encephalopathy in diabetes. Phytomedicine, 91: 153686-153699. DOI: 10.1016/j.phymed.2021.153686.

29. Babaei P, Eyvani K and Kouhestani S (2021): Sex-Independent Cognition Improvement in Response to Kaempferol in the Model of Sporadic Alzheimer's Disease. Neurochem Res, 46(6): 1480-1486. DOI: 10.1007/s11064-021-03289-y.

30. Shigematsu K, Takeda T, Komori N, Tahara K and Yamagishi H (2021): Hypothesis: Intravenous administration of mesenchymal stem cells is effective in the treatment of Alzheimer's disease. Med Hypotheses, 150: 110572-110574. DOI: 10.1016/j.mehy.2021.110572.

31. Xu H and Van Remmen H (2021): The SarcoEndoplasmic Reticulum Calcium ATPase (SERCA) pump: a potential target for intervention in aging and skeletal muscle pathologies. Skelet Muscle, 11(1): 25-33. DOI: 10.1186/s13395-021-00280-7.

32. Wu Y, Zhang C, Guo R, Wu D, Shi J, Li L, Chu Y, Yuan X and Gao J (2021): Mesenchymal Stem Cells: An Overview of Their Potential in Cell-Based Therapy for Diabetic Nephropathy. Stem Cells Int, 2021: 6620811-6620822. DOI: 10.1155/2021/6620811.

33. Zhang IX, Raghavan M and Satin LS (2020): The Endoplasmic Reticulum and Calcium Homeostasis in Pancreatic Beta Cells. Endocrinology, 161(2): 28-65. DOI: 10.1210/endocr/bqz028.

34. Luebke JI, Weaver CM, Rocher AB, Rodriguez A, Crimins JL, Dickstein DL, Wearne SL and Hof PR (2010): Dendritic vulnerability in neurodegenerative disease: insights from analyses of cortical pyramidal neurons in transgenic mouse models. Brain Struct Funct, 214(2): 181–199. DOI: 10.1007/s00429-010-0244-2.

35. Ali AA, Khalil MG, Abd El-Latif DM, Okda T, Abdelaziz AI, Abu-Elfotuh K, Kamal MM, Wahid A (2022): The influence of vinpocetine alone or in combination with Epigallocatechin-3-gallate, Coenzyme COQ10, Vitamin E and Selenium as a potential neuroprotective combination against aluminium-induced Alzheimer's disease in Wistar Albino Rats. Arch Gerontol Geriatr, 98: 104557-104567. DOI: 10.1016/j.archger.2021.104557.

36. Więckowska-Gacek A, Mietelska-Porowska A, Wydrych M and Wojda U (2021): Western diet as a trigger of Alzheimer's disease: From metabolic syndrome and systemic inflammation to neuroinflammation and neurodegeneration. Ageing Res Rev, 70: 101397-101419. DOI: 10.1016/j.arr.2021.101397.

37. Bagheri-Mohammadi S (2021): Stem cell-based therapy as a promising approach in Alzheimer's disease: current perspectives on novel treatment. Cell Tissue Bank, 22(3): 339-353. DOI: 10.1007/s10561-020-09896-3.

38. Puranik N, Yadav D, Chauhan PS, Kwak M and Jin JO (2021): Exploring the Role of Gene Therapy for Neurological Disorders. Curr Gene Ther, 21(1): 11-22. DOI: 10.2174/1566523220999200917114101.

39. Chami M and Checler F (2020): Alterations of the Endoplasmic Reticulum (ER) Calcium Signaling Molecular Components in Alzheimer's Disease. Cells, 9(12): 2577-2599. DOI: 10.3390/cells9122577.

40. Jeong H, Kim OJ, Oh SH, Lee S, Reum Lee HA, Lee KO, Lee BY and Kim NK (2021): Extracellular Vesicles Released from Neprilysin Gene-Modified Human Umbilical Cord-Derived Mesenchymal Stem Cell Enhance Therapeutic Effects in an Alzheimer's Disease Animal Model. Stem Cells Int, 2021: 5548630-5548649. DOI: 10.1155/2021/5548630.

41. Solana-Manrique C, Muñoz-Soriano V, Sanz FJ and Paricio N (2021): Oxidative modification impairs SERCA activity in Drosophila and human cell models of Parkinson's disease. Biochim Biophys Acta Mol Basis Dis, 1867(7): 166152-166163. DOI: 10.1016/j.bbadis.2021.166152.

42. Kim SH, Kim JY, Park SY, Jeong WT, Kim JM, Bae SH and Kim GJ (2021): Activation of the EGFR-PI3K-CaM pathway by PRL-1-overexpressing placenta-derived mesenchymal stem cells ameliorates liver cirrhosis via ER stress-dependent calcium. Stem Cell Res Ther, 12(1): 551-564. DOI: 10.1186/s13287-021-02616-y.

43. Zhang R, Li C, Du R, Yuan Y, Zhao B, Zhang Y and Wang C (2022): Mesenchymal stem cells: As a multi-target cell therapy for clearing β-amyloid deposition in Alzheimer’s disease. BIOCELL, 46(3): 583-592. DOI: 10.32604/biocell.2022.017248.

44. Aboulhoda BE, Rashed LA, Ahmed H, Obaya EMM, Ibrahim W, Alkafass MAL, Abd El-Aal SA and ShamsEldeen AM (2021): Hydrogen sulfide and mesenchymal stem cells-extracted microvesicles attenuate LPS-induced Alzheimer's disease. J Cell Physiol, 236(8): 5994-6010. DOI: 10.1002/jcp.30283.

45. Angelova PR (2021): Sources and triggers of oxidative damage in neurodegeneration. Free Radic Biol Med, 173: 52-63. DOI: 10.1016/j.freeradbiomed.2021.07.003.

**الملخص العربى**

# التأثير العلاجي المحتمل للخلايا الجذعية المعدلة جينيا مقابل الخلايا الجذعية غير المعدلة في الحصين و قشرة المخ في نموذج الجرذان البيضاء الأنثوية لمرض الزهايمر الناتج عن مرض السكري النوع الأول المحدث تجريبيا

**مها بليغ زكري[١،٢]، هالة جبر متولي[٣]، أميمة محمد عبد الواحد[٤]، مي عبد العزيز جودة[٥،٦]، رقية محمد حسن[١]، شيماء أحمد زكي[١]، الشيماء جمال أبو الخير[١]**

**[١]قسم الهستولوجيا الطبية وبيولوجيا الخلية ، كلية الطب ، جامعة القاهرة**

**[٢]كلية طب الفم والأسنان ، جامعة المستقبل ، مصر**

**[٣]قسم الباثولوجيا الإكلينيكية بكلية الطب جامعة القاهرة**

**[٤]قسم الفسيولوجيا الطبية بكلية الطب جامعة القاهرة**

**قسم الكيمياء الحيوية الطبية والبيولوجيا الجزيئية ، كلية الطب ، جامعة القاهرة[٥]، مصر ، جامعة بدر بالقاهرة[٦]**

**الخلفية والأهداف:** تم تسجيل العلاقة بين مرض السكري من النوع الأول ومرض الزهايمر. في الآونة الأخيرة ، تم الاهتمام على نطاق واسع بالتعديل الجيني للخلايا الجذعية . هدف العمل الحالي لتقييم التأثير العلاجي المحتمل للخلايا الجذعية المعدلة جينيًا على قشرة المخ والحصين في مرض الزهايمر الناتج عن مرض السكري النوع الأول.

**الطرق والنتائج:** تم تقسيم ٤٠ من اناث الجرذان إلى: مجموعة الدراسة في المختبر: ٤ جرذان استخدمت لاستزراع وتكثيف الخلايا الجذعية وتحضير سيركا ٢ب. المجموعة الضابطة (أ) : ٦ فئران . مجموعة السكري (ب): ١٠جرذان تم حقنها داخل غشاء البطن بالاستربتوزوتوسين بجرعة ٥٠ مللي/ كجم. مجموعة الخلايا الجذعية الغير تعدائية (ج): ١٠ فئران ،حيث تلقت ١ × ١٠٦ من الخلايا الجذعية حقنا في الوريد. مجموعة الخلايا الجذعية التعدائية بجين السيركا ٢ب (د): حقنت ١٠ جرذان بجرعة ١× ١٠٦ من الخلايا الجذعية التعدائية. بعد ٥٢ يومًا بعد إثبات حدوث السكري ، أجريت الدراسات العصبية ، السيرولوجية ، النسيجية ، الشكلية ، تفاعل البوليميراز المتسلسل ، اللطخة الغربية ودراسات الكيمياء الحيوية. أظهرت الدراسة العصبية انخفاضًا كبيرًا ذو دلالة إحصائية في المجموعة (ب) والمجموعة (ج). قامت المجموعة (ب) بتوضيح الخلايا العصبية المتدهورة في طبقة هرمية خارجية لقشرة المخ و طبقة التلفيف المسنن للحصين. كشفت المجموعة (د) عن انحدار أكثر وضوحًا للتغيرات التفسخية عن المجموعة (ج). تم العثور على زيادة كبيرة ذي دلالة إحصائية في متوسط مساحة الخلايا العصبية المشوهة والخلايا العصبية المصبوغة بواسطة صبغة الكونجو الأحمر ، ومتوسط النسبة المئوية من تفاعلات مناعية في المجموعتين (ب) و(ج). كما عبر متوسط تركيز أيون الكالسيوم ، والكاتلاز ، والقيم المتوسطة لجين وبروتين السيركا ٢ب عن انخفاض كبير ذو دلالة إحصائية في المجموعتين (ب) و(ج). وأظهرت القيم المتوسطة لل ام دي اي و البيتا أميلويد بروتين زيادة كبيرة ذات دلالة إحصائية في المجموعتين (ب) و(ج).

**الاستنتاجات:** أثبتت الخلايا الجذعية المعدلة جينيًا بالجين الساركوبلازمي لشبكة الكالسيوم ATPase٢b تأثير علاجي واضح مما يشير إلى فعاليتها وقدرتها على التجدد في التحسن الملحوظ لمرض الزهايمر الناتج عن مرض السكري النوع الاول.